Load Tests on Post-Tensioned Pavement Slabs

A. P. CHRISTENSEN
Development Engineer, Research and Development Laboratories, Portland Cement Association, Skokie, Illinois

This paper reports data from static load tests conducted on three concrete slabs post-tensioned with steel strands. Each slab was 30 ft long, 12 ft wide, and 5 in. thick. The principal variable was the amount of prestress. Two slabs had only longitudinal prestress, one of 180 psi and the other of 360 psi. The third slab had 360 psi longitudinal prestress and 70 psi transverse prestress.

Data from interior loadings indicated that transverse prestress may be required to prevent bottom surface cracks from extending to the top surface. This suggests that if the structural contribution of prestressing is to be utilized fully both longitudinal and transverse prestress may be required for airport paving. For edge loadings none of the bottom surface cracks extended to the top. This suggests that longitudinal prestress may be sufficient for highway pavements.

These comments on the mode of failure are based on static load tests using one dual-plate assembly to simulate a dual-tire wheel load.

•PRESTRESSED concrete pavements have been constructed in many localities during the past 15 years. Prestress application methods may be classified into two groups. One group utilized either post-tensioned or pretensioned steel cables placed in long individual slabs; the other group utilized either expanding flat jacks or wedges placed in the joints between long slabs with the reactions absorbed by end abutments. Useful information has been reported concerning the relative merits of construction methods, but little data have been developed on which a rational method of design can be based.

The principal items of uncertainty concern the behavior of a prestressed concrete pavement when loaded and the mode of failure. In some of the early discussions of these items, the limiting load on a prestressed concrete pavement was related only to cracking in the bottom surface of the slab. The increase in load-carrying capacity attained by prestressing would then be only the amount which the prestress added to the flexural strength of the pavement. Subsequent studies (1, 2) have shown a much greater increase in load-carrying capacity, and the occurrence of top surface cracking has been suggested as the criterion for failure. In the design of a prestressed concrete pavement with the top surface cracking failure concept, it is necessary to determine stresses and deflections beyond conditions to which the elastic theory is applicable. To provide a better understanding of the stresses and deflections that develop in a prestressed concrete pavement when loads are applied after the occurrence of bottom surface cracking, load tests were conducted on three prestressed concrete slabs constructed at the Portland Cement Association (PCA) Research and Development Laboratories.

SCOPE AND OBJECTIVES

Three concrete slabs were constructed in an outdoor environment and were prestressed with post-tensioned steel strands. Each slab was 30 ft long, 12 ft wide, and

Paper sponsored by Committee on Rigid Pavement Design.

5 in. thick. The slab cross-sections were selected to be suitable for highway design. A thickness of 5 in. has been used for prestressed concrete highways in other experimental installations, and a width of 12 ft corresponds to a highway traffic lane. The length of 30 ft was sufficient to allow the development of moments equal to those in a pavement of infinite length when loaded at edge locations.

The amount and direction of prestress were varied for the three slabs. Two of the slabs had only longitudinal prestress, one of 180 psi and the other of 360 psi. The third slab had 360 psi longitudinal prestress and 70 psi transverse prestress. Static loads were applied at both interior and edge locations with magnitudes sufficient to determine slab deflection and moment characteristics in both the elastic and plastic range. Measurements were made to determine strain and deflection profiles of the slab and the pressure on the subgrade.

Specific Objectives

The objectives of the program are (a) to determine the effect of prestress level on strains and deflections causing bottom and top surface cracking for edge and interior loading, and (b) to interpret the significance of these data relative to the criterion for failure of a prestressed pavement.

MATERIALS AND PREPARATION

The slabs were constructed in an outdoor environment with the following materials and preparation.

Subgrade Material

The subgrade material for all slabs was a sandy clay loam with an AASHO classification of A-4. Subgrade characteristics are given in Table 1.

The subgrade modulus was determined from plate bearing tests made prior to the construction of each slab. The average value of Westergaard's subgrade modulus, k, as determined with a 30-in. diameter plate at 0.05-in. deflection was 140 pci.

Friction Reducing Layer

A friction reducing layer was used under all slabs to reduce to a minimum stresses resulting from restraint to horizontal slab movement. This layer consisted of $\frac{1}{4}$ in. of fine uniform sand covered with waterproof paper. All of the sand passed the No. 30 sieve, 30 percent passed No. 50, and all was retained on No. 100. The sand was compacted at its optimum moisture content by hand tamping.

Steel Prestressing Strand and Conduit

The post-tensioning strands were composed of uncoated stress-relieved steel wires. Dimensions and properties were diameter, $\frac{7}{16}$ in.; area, 0.1089 sq in.; minimum ult. str., 27,000 lb; and approx. mod. of elast. 26,000,000 psi.

Openings for the strands were provided by $\frac{3}{4}$ in. I.D. flexible conduit made from interlocking 0.010-in.-thick strip steel. As shown in Figure 1, the longitudinal conduit was placed at the slab mid-depth. For the slab with transverse prestress, the transverse conduit was placed alternately above and below the longitudinal conduit.

TABLE 1

SUBGRADE PROPERTIES

	Particle Size (mm)	Percent	Pcf	Pci
Material				
Gravel	76.2 -2.0	1	-	-
Coarse sand	2.0 -0.42	6	-	-
Fine sand	0.42 -0.074	41	-	-
Silt	0.074-0.005	27	-	-
Clay	below 0.005	25	-	-
Liquid limit	-	23.1	-	-
Plasticity index	-	7.3	-	-
Maximum dry density (AASHO stand)	-	-	114.5	-
Optimum moisture	-	13.2	-	-
Modulus of subgrade reaction, k	-	-	-	140

Concrete Slabs

The concrete mix used for the three test slabs contained 564 lb of cement per cu yd; water-cement ratio was 0.48 by

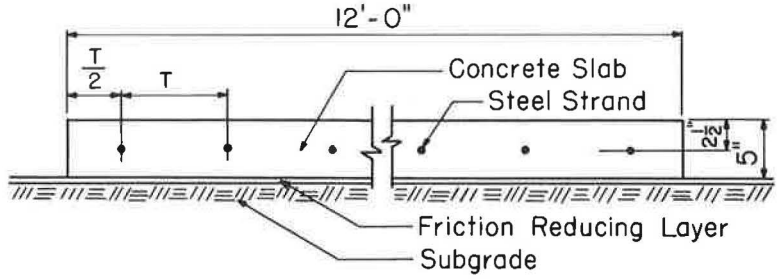

Transverse Section (All Slabs)

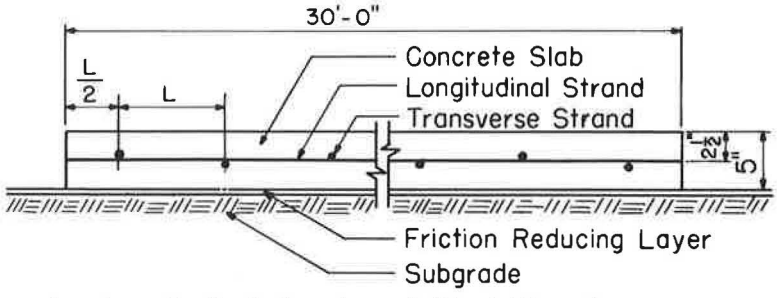

Longitudinal Section (Slab 3 Only)

Figure 1. Prestressed concrete slab cross-sections.

weight; maximum size gravel aggregate was 1½ in., and the sand-aggregate ratio was 37 percent by weight. The slump averaged 4 in., and the air content averaged 5 percent.

Beams, 6 by 6 by 30 in., were made at the time of casting and were tested after 28 days of moist curing at 73 F and 100 percent relative humidity. In addition, data were obtained from 5-in. wide beams cut from the slabs after load testing was completed. The concrete properties as determined from these beams are shown in Table 2. For computing stresses from measured strains, a value of 5 million psi was used for the concrete modulus of elasticity for each test slab.

During placing of the concrete steel chairs were used to keep the conduits at the required depth, and ⅝-in. diameter deformed reinforcing bars were inserted through the conduits prior to casting to provide greater rigidity against bending. For Slabs 1 and 2, a wood spacer that was notched at the proper steel locations was moved ahead of the concrete as it was placed. In Slab 3 with transverse pre-

TABLE 2

CONCRETE PROPERTIES

Slab No.	A-Beams[1]		B-Beams[2]	
	Mod. of Rupture (psi)	Sonic Modulus (10^6 psi)	Mod. of Rupture (psi)	Sonic Modulus (10^6 psi)
1	580	5.06	700	6.14
2	520	4.70	640	5.75
3	540	4.61	660	5.88

[1]A-Beams (6 by 6 by 30 in.) made at time of casting and tested after 28 day moist curing.
[2]B-Beams (5 by 5 by 30 in.) cut from slabs after load testing was completed at an average period of 15 months after construction.

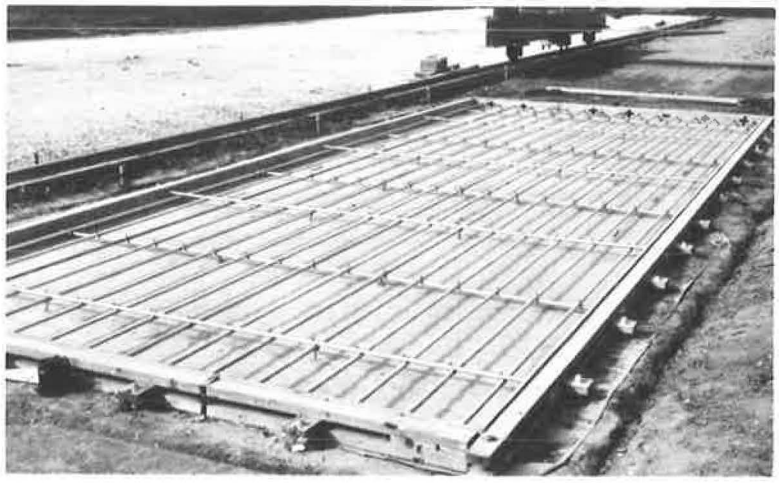

Figure 2. Grid of flexible conduit prepared for slab with two-way prestress.

TABLE 3
PRESTRESSING VALUES

Slab No.	Steel Spacing (in.)		Concrete Prestress (psi)	
	Longitudinal	Transverse	Longitudinal	Transverse
1	18	0	180	0
2	9	0	360	0
3	9	45	360	70

stressing, the longitudinal conduits were tied to the transverse conduits as shown in Figure 2. All of the methods used to keep the conduits in alignment were judged to be satisfactory because the losses from friction between the strands and the conduits were negligible during tensioning.

Prestressing and Grouting

After the concrete had cured for a minimum of 28 days, the slabs were prestressed. Before inserting the steel strands, the conduits were cleaned with water and air under pressure. The strands were stressed individually using a hydraulic ram at one end of the slab. They were held at the required stress by means of a grip at each end. The load on each strand was carefully measured using a load transducer (3) between the strand grip and the concrete slab.

After stressing each strand to 150,000 psi or 16,290 lb, the conduits were filled with grout. A minimum period of 24 hr elapsed between stressing and grouting, and the stress on each strand was adjusted if necessary just prior to grouting. The spacing of the steel strands and the magnitude of concrete prestress for each slab are given in Table 3.

The grout consisted of neat cement with a water-cement ratio of 0.5 by weight. Aluminum powder in the amount of 2.0 gm per 100 lb of cement was added to reduce shrinkage.

LOADING DEVICES

Loads were applied to the slabs by a 50-ton hydraulic ram reacting against a steel beam as shown in Figure 3. Rails on each side of the test area for the entire length facilitated the positioning of the steel beam. This beam was held in position during a load test by soil anchors spaced along the rails permitting the application of loads up to 100,000 lb.

Loads were applied through two plates in the shape of rectangles with semicircular ends simulating dual tires. Each plate had an area of 100 sq in. with a length of 13.83 in. and a width of 8.30 in. During load testing the plates were spaced 13.0 in. apart measured between the centerlines. The magnitude of load was measured by a pair of transducers (3) with electrical response sensed by strain indicators.

Figure 3. Outdoor test area showing the loading device.

INSTRUMENTATION

The instrumentation plan was not the same at all test locations. Instrumentation was provided to measure strain and deflection of the concrete slab and pressure on the subgrade at various load increments.

Strain measurements were made using 6 in. long SR-4 type A9 gages cemented to the concrete at a number of top surface and vertical edge locations. Deflections were measured with 0.001-in. dial indicators attached to a wooden bridge that was supported independently of the slab. Pressures at the top of the subgrade during edge load tests were measured with Carlson stress meters (4). These meters had a $7\frac{1}{4}$-in. diaphragm plate and were installed in a mortar bed with the stem downward. A length of sponge rubber weather stripping material was wrapped around the circumference of the diaphragm to assure unrestricted action. Instrument constants were furnished by the manufacturer, and check tests on the calibration curve were made after the stress meter had been installed.

EDGE LOAD TESTS

Static loads were applied at the longitudinal slab edges. The dual loading plates were positioned with the outer edge of one of the plates tangent to the longitudinal edge of the slab at a minimum distance of 10 ft from a transverse edge. Loads applied along one edge of each slab were sufficient to cause only bottom surface cracking. Along the opposite edge the loads were sufficient to cause top surface cracking. In this way the response of the test slabs to load was determined after a number of either bottom or top surface cracks had formed.

Bottom Surface Cracking

The magnitude of load causing bottom surface cracking was determined from strain and deflection data obtained during an initial load test on each slab. The initial load was applied at a longitudinal edge midway between slab ends. After application and release of the initial load, loads of the same maximum magnitude were applied both at the initial location and also at 6-in. intervals for a distance of 2 ft along the edge. Sufficient time elapsed between each load application to permit recovery of the slab and subgrade.

Loads were applied in 4-kip increments at the positions shown in Figure 4 with measurements made at each increment to determine compressive strain, tensile strain, and deflection at the load.

Initial Loadings.—The data obtained from the initial edge load tests on the three slabs are shown in Figures 5 through 7. The slabs were uncracked at the time of loading. Figure 5 shows the strains measured by the gage on the top surface and the gage on the vertical edge near the bottom surface of each slab. A linear strain distribution was assumed, and straight lines connecting these measured strains passed through zero strain near the mid-depth of the slabs before bottom surface cracking occurred. After cracking there were larger strain changes per unit load; the strains measured near the bottom surface increased more than the top surface strains, and the locations of zero strain occurred above the mid-depth of the slabs. The true bottom surface cracking loads were difficult to determine but were estimated at 18,000 lb for Slab 1 and 20,000 lb for Slabs 2 and 3. The additional longitudinal prestress resulted in an increase in the load causing bottom surface cracks that extended in a generally transverse direction inward from the edge.

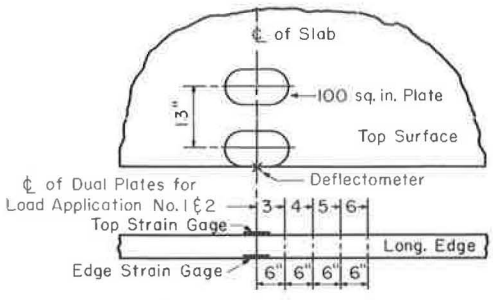

Figure 4. Bottom cracking load positions and instrumentation.

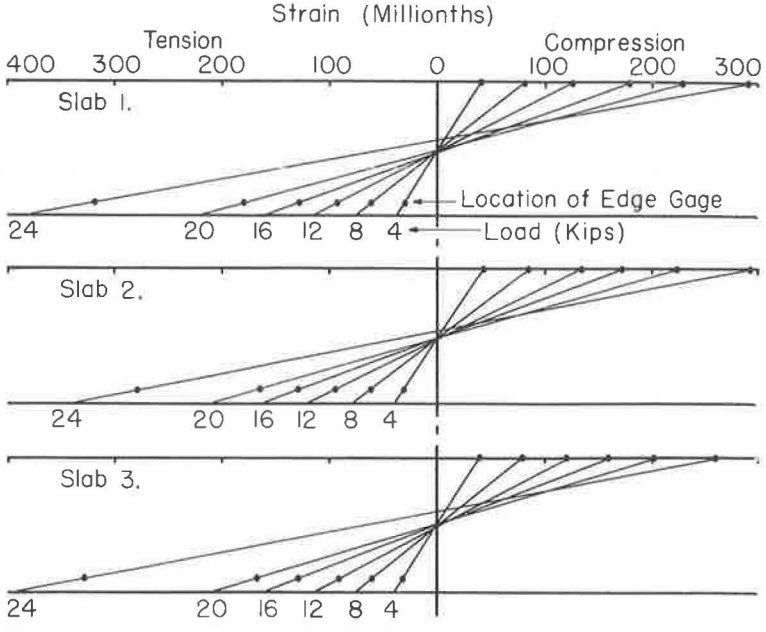

Figure 5. Edge strain diagrams.

Top surface longitudinal edge stresses at the load were computed by multiplying the measured compressive strains by the concrete elastic modulus using a value of 5 million psi. These stresses are shown in Figure 6 with the corresponding edge deflections shown in Figure 7. These figures indicate that the compressive stress and deflection at the edge were nearly proportional to the applied load before bottom surface cracking occurred. Values computed by methods based on the elastic theory are also shown on these figures. For this purpose, influence charts (5) were used with a value of 140 pci for the subgrade modulus, 5 million psi for the concrete elastic modulus, and 0.15 for Poisson's ratio. The load test compressive stresses and deflections averaged 16 per-

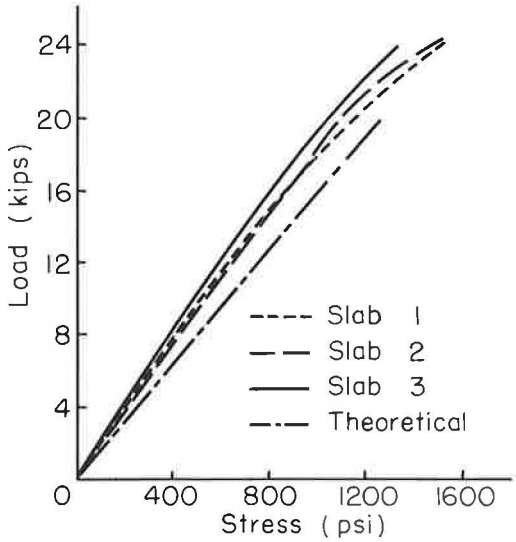

Figure 6. Top surface compressive edge stresses.

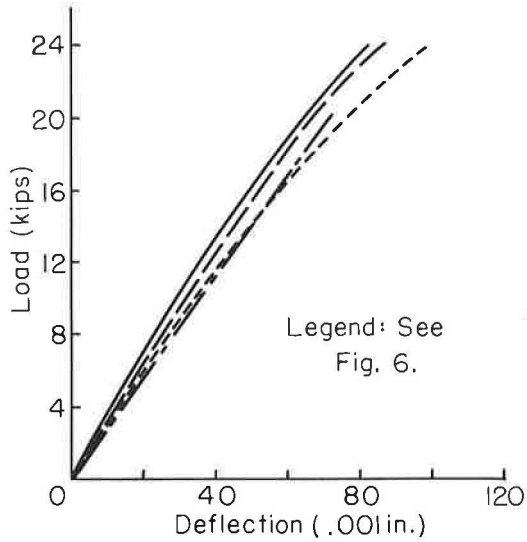

Figure 7. Edge deflections.

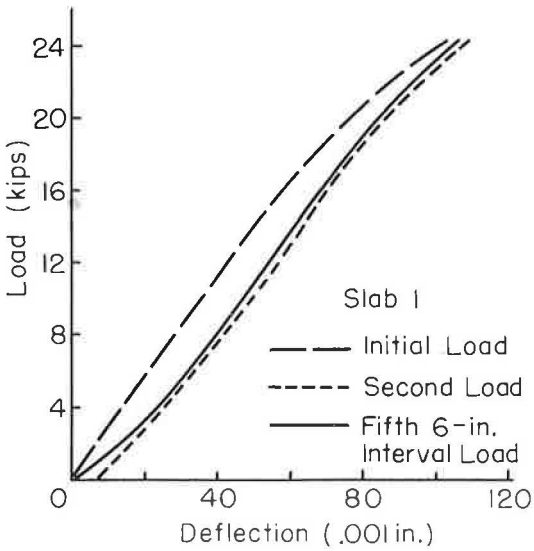

Figure 8. Edge deflections.

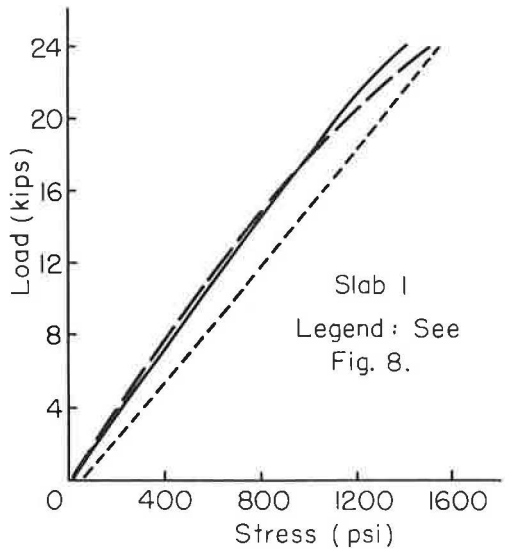

Figure 9. Top surface compressive edge stresses.

cent and 5 percent, respectively, less than the theoretical values before cracking occurred.

Second and Interval Loadings.—The maximum load initially applied on each of the three slabs was 24 kips. This load was also maximum for the second application of load at the initial location and for loads applied successively at 6-in. intervals along the edge of each cracked slab. The results from the second load application and the fifth 6-in. interval load application on Slab 1 are shown in Figures 8 and 9.

The data from the second load application on Slab 1 are representative of those obtained from tests on all three slabs after bottom cracking had occurred. Residual deflection was measured after each load was applied and released. Only residual edge deflection after the initial load was released is reported as shown by the no load deflection of the second load curve in Figure 8. Averaging the data for the three slabs, the residual deflections were 5 percent of the initial 24-kip load deflections. During the second load application on the three slabs, the ratios of deflection to load were nearly constant throughout the entire range from the residual values at no load to values at the 24-kip load that were about 5 percent greater than those resulting from the initial load applications. As shown in Figure 9, the ratio of compressive stress to load was also nearly constant throughout the entire range of the second application. The stresses in the three slabs at loads of 24 kips averaged 3 percent greater during the second load application than during the initial application.

The data from the load tests at 6-in. intervals showed variations due to small differences in the distance between bottom surface cracks. The results of the fifth 6-in. interval load application on Slab 1 as shown in Figures 8 and 9 are typical of most of the tests. As shown in Figure 8, the deflections for the interval and second load applications were similar. The deflections of the three slabs at 24 kips averaged 4 percent greater for the interval applications than for the initial applications.

Of special interest during the 6-in. interval applications were the loads causing the development of new bottom surface cracks as determined from the edge stresses. As shown by Figure 9, the top surface longitudinal edge stresses at the load location were similar during the initial and interval load applications. However, the strains measured on the vertical edge near the bottom surface were slightly smaller during the interval applications than during the initial applications. There was probably some stress relief due to the proximity of bottom cracking. As a result, the loads causing bottom surface cracking during the 6-in. interval applications were usually larger by as much as 10 percent than those determined during the initial applications.

Top Surface Cracking

The initial load for each series of top surface cracking studies was applied midway between the slab ends at the opposite side from that tested for bottom surface cracking. The load was increased until top surface cracking was observed. After application and release of the initial load, a second load of the same maximum magnitude was applied at the initial location. Loads of a slightly greater magnitude were then applied at 6-in. intervals along the edge for a distance of 2 ft and continued at intervals of 1 ft for 3 ft more. Sufficient time elapsed between each load application to permit recovery of the slab and subgrade.

Loads were applied in 4-kip increments at the positions shown in Figure 10. Measurements were made at each increment to determine the longitudinal and transverse concrete strain and deflection profiles and the maximum intensity of pressure on the subgrade. The location of the top surface crack was also determined if one occurred.

Initial Loadings.—To illustrate the type of strain data obtained during these load tests, the results of the initial top surface cracking edge load test on Slab 1 are shown in Figures 11 and 12. Figure 11 shows the distribution of longitudinal strains measured on the top surface of the slab along the edge. Figure 12 shows the distribution of transverse and longitudinal strains measured on the top surface of the slab along the transverse center line of the loaded area.

These measured strains were used in the computation of stresses by the following equations:

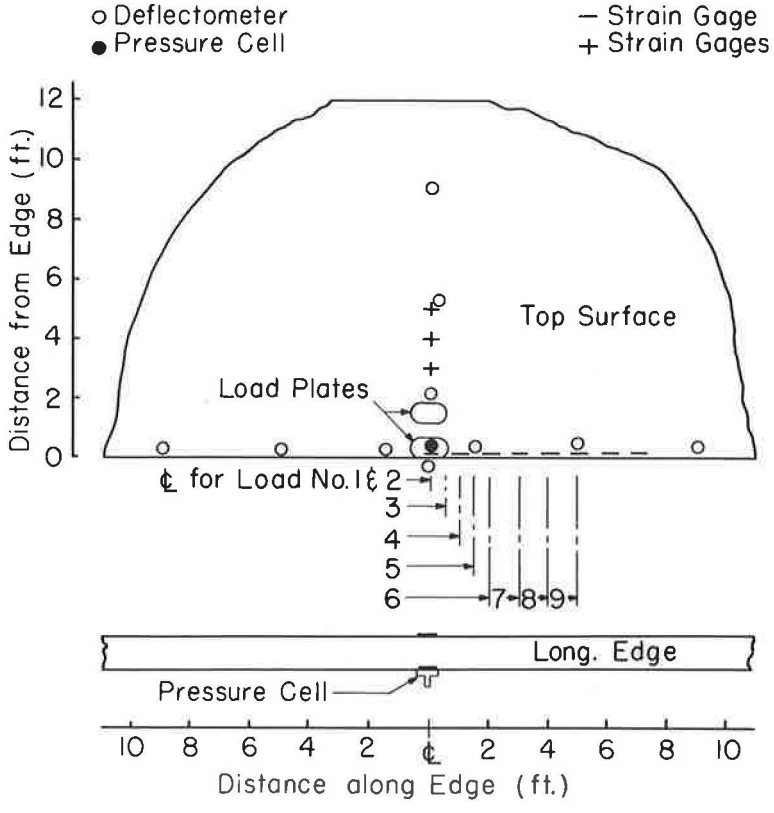

Figure 10. Top surface cracking load positions and instrumentation.

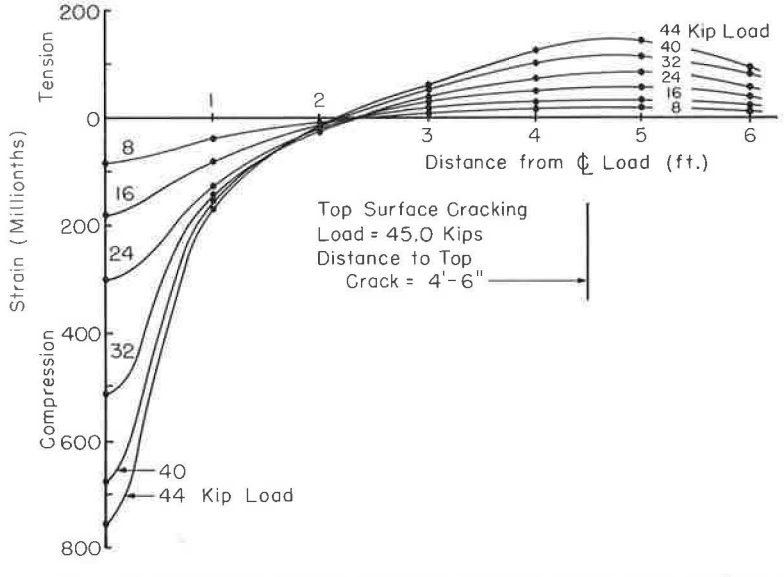

Figure 11. Distribution of top surface strains along edge of Slab 1.

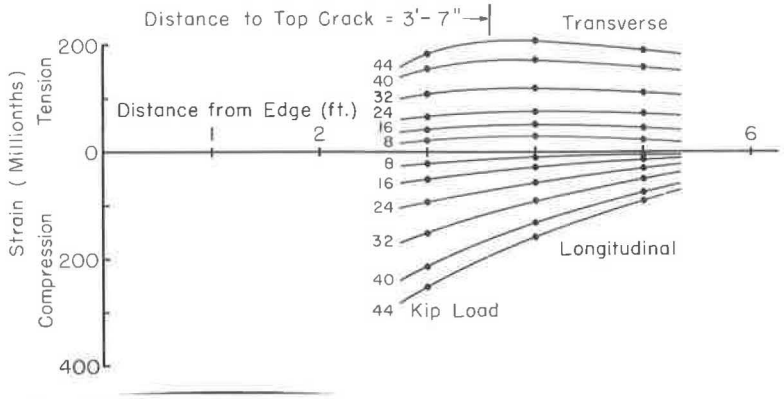

Figure 12. Distribution of top surface strains inward from edge of Slab 1.

$$\sigma_x = \frac{E}{1 - \mu^2} (e_x + \mu\ e_y) \quad (1)$$

$$\sigma_y = \frac{E}{1 - \mu^2} (e_y + \mu\ e_x) \quad (2)$$

in which

σ_x = longitudinal stress (psi),
σ_y = transverse stress (psi),
e_x = longitudinal strain (in./in.),
e_y = transverse strain (in./in.),
E = concrete elastic modulus (5,000,000 psi), and
μ = Poisson's ratio assumed as 0.15.

The maximum top surface tensile stresses in a longitudinal direction at the edge and in a transverse direction inward from the edge are shown in Figures 13 and 14, respec-

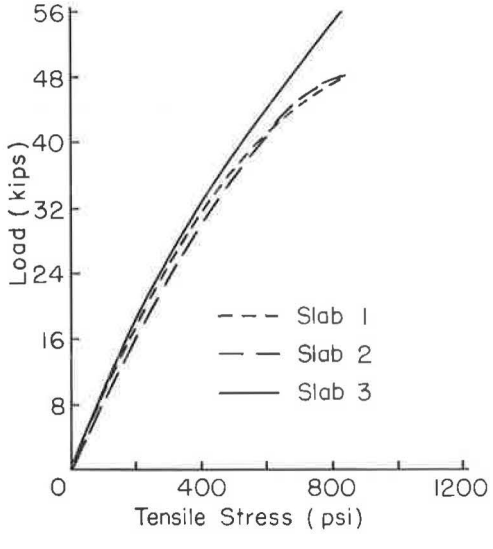

Figure 13. Maximum top longitudinal tension along edge.

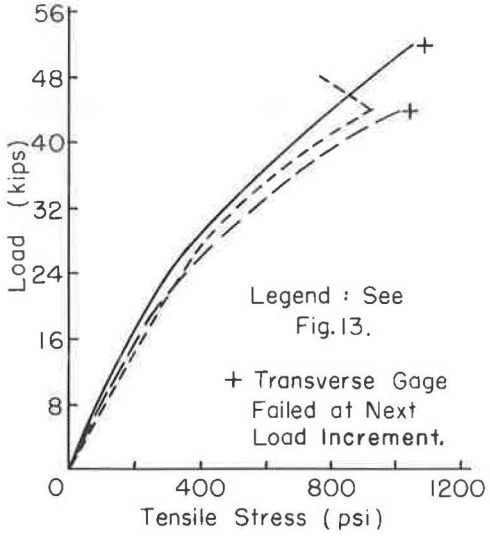

Figure 14. Maximum top transverse tension inward from edge.

tively. The maximum tensile stresses inward from the edge averaged 14 percent greater than those at the edge. When these tensile stresses were equal to the cracking stresses of the prestressed slabs, top surface cracking occurred.

From visual observations made during load testing, the top surface cracks appeared to form initially in the longitudinal direction at distances varying from 43 to 52 in. inward from the edge. With the top surface cracking load maintained, the crack progressed toward the edge of the slab. Top cracks occurred within 6 in. of the location of the maximum reading strain gage for load tests on all three slabs. The magnitude of load causing top surface cracking and the location of the cracks for the three test slabs are given in Table 4. The top cracking load was greatest for Slab 3 with both longitudinal and transverse prestress.

Top surface longitudinal compressive edge stresses and edge deflection at the transverse centerline of the loaded area are shown in Figures 15 and 16, respectively. When bottom surface cracking occurred, there was a slight increase in the rate of deflection change per unit load. When top surface cracking occurred, there was a relatively large increase in deflection at the load. Typical deflection profiles are shown in Figure 17 for increments of edge load on Slab 1. The distances from the load to the location of zero deflection were similar for all slabs and varied from about 8 to 10 ft.

The maximum subgrade pressures are shown in Figure 18. The slopes of these load pressure curves for the linear portions from 12 to 24 kips were used with load deflection ratios determined from Figure 16 for the same loading range to compute values of k. The computed values averaged 129 pci for the three slabs as compared with the value of 140 pci determined from plate bearing tests.

TABLE 4

TOP SURFACE CRACKING LOADS AND LOCATIONS OF CRACKS

Slab No.	Top Surface Cracking Load (kips)	Distance to Top Surface Crack (in.)		
		A	B	C
1	45.0	52	54	43
2	45.0	80	94	52
3	54.0	66	58	46

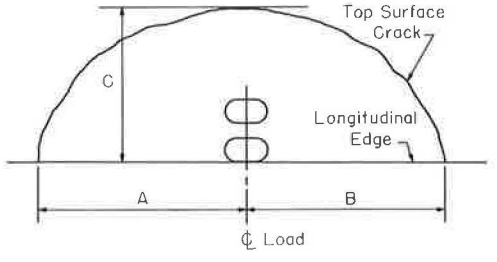

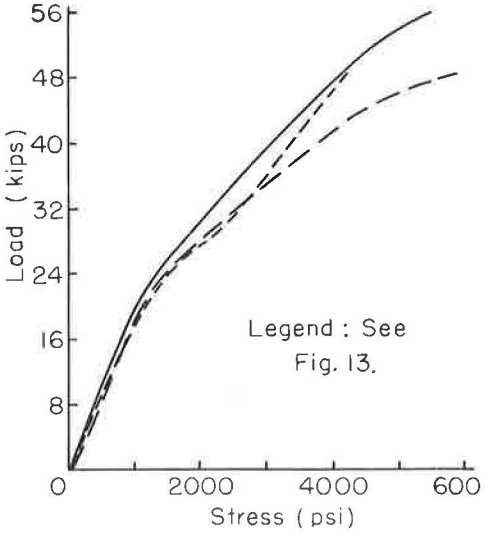

Figure 15. Top surface longitudinal compressive edge stress at load.

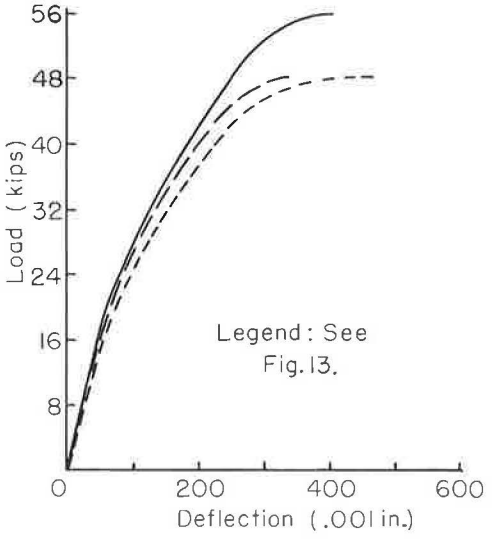

Figure 16. Edge deflections at load.

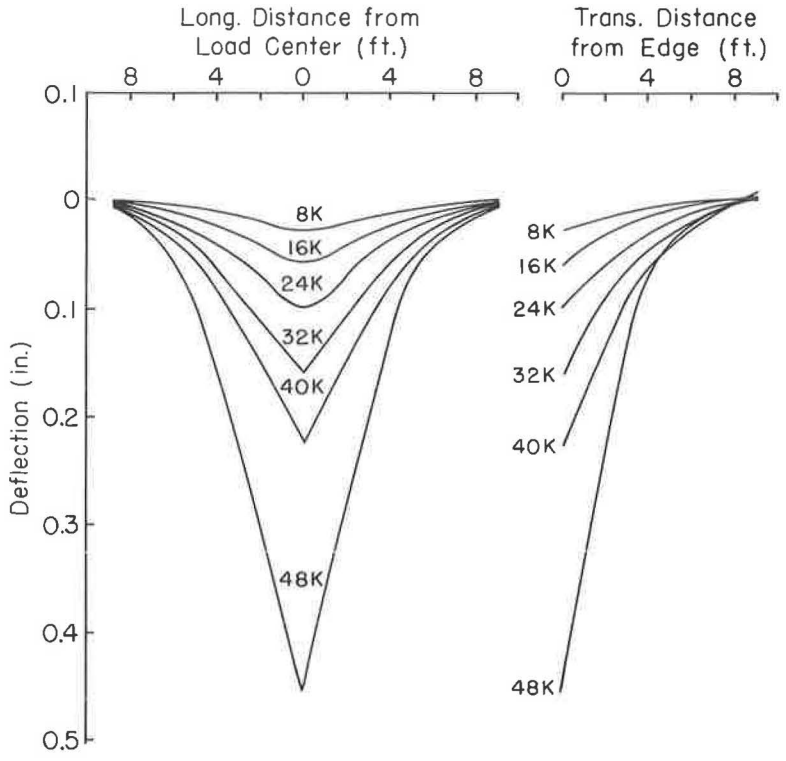

Figure 17. Typical deflection profiles, initial load, Slab 1.

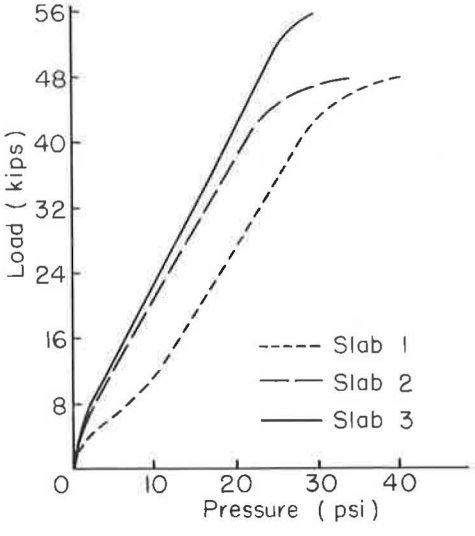

Figure 18. Maximum subgrade pressure at load.

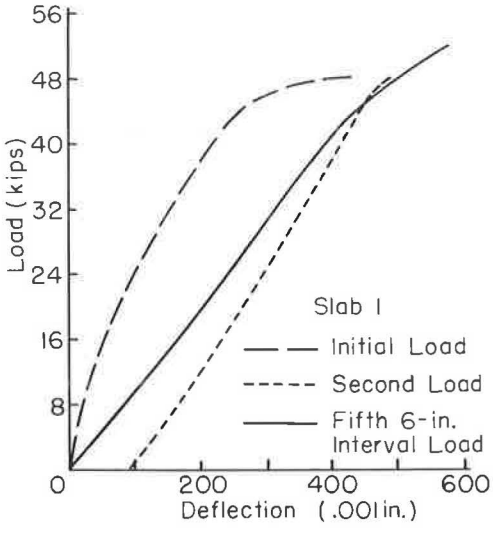

Figure 19. Edge deflection at load.

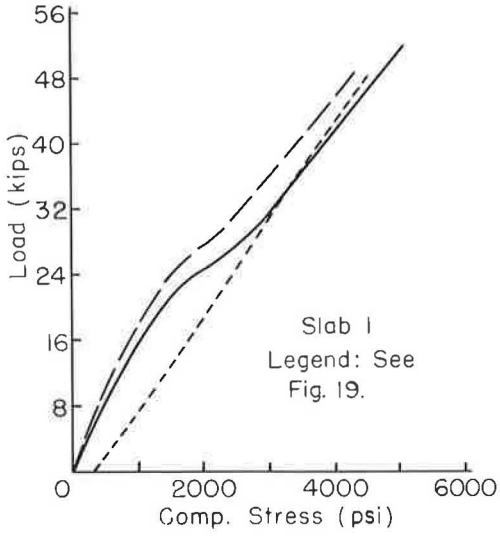

Figure 20. Top surface compressive edge stress at load.

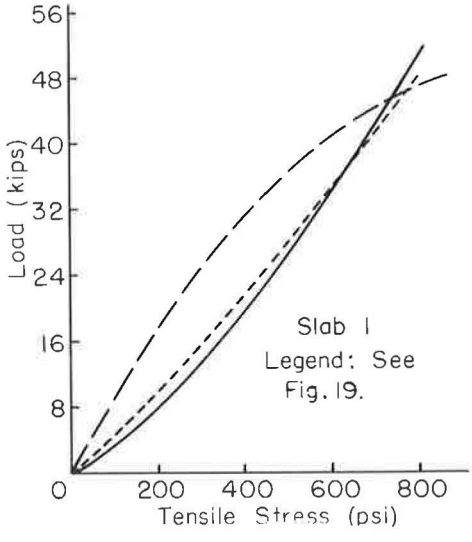

Figure 21. Maximum top surface longitudinal tension along edge.

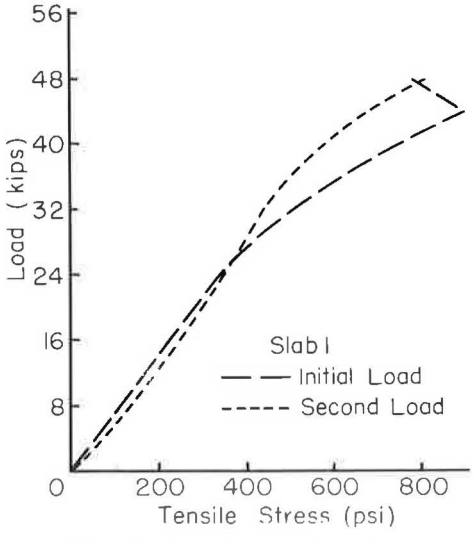

Figure 22. Maximum top surface transverse tension inward from edge.

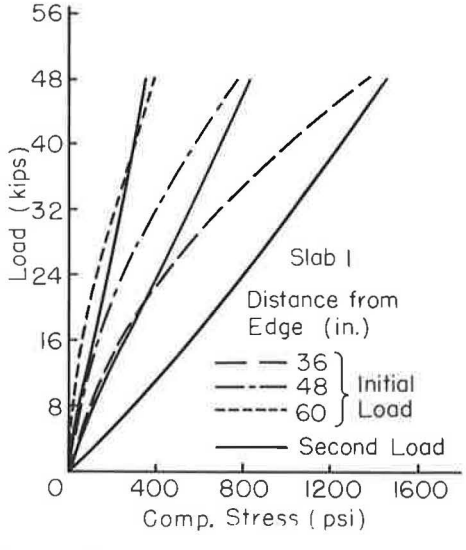

Figure 23. Top surface longitudinal compressive stress inward from edge.

Second Loadings.—The maximum top surface cracking loads initially applied were 48, 48, and 56 kips for Slabs 1, 2, and 3, respectively. The same maximum loads were used for the second applications on the three slabs at the initial locations. The results from the second load application on Slab 1 as shown in Figures 19 to 23 were representative of those obtained from tests on all three slabs after top cracking had occurred.

After the initial load was removed some residual deflections remained in the slabs. The largest residual deflection occurred at the location of maximum deflection on the

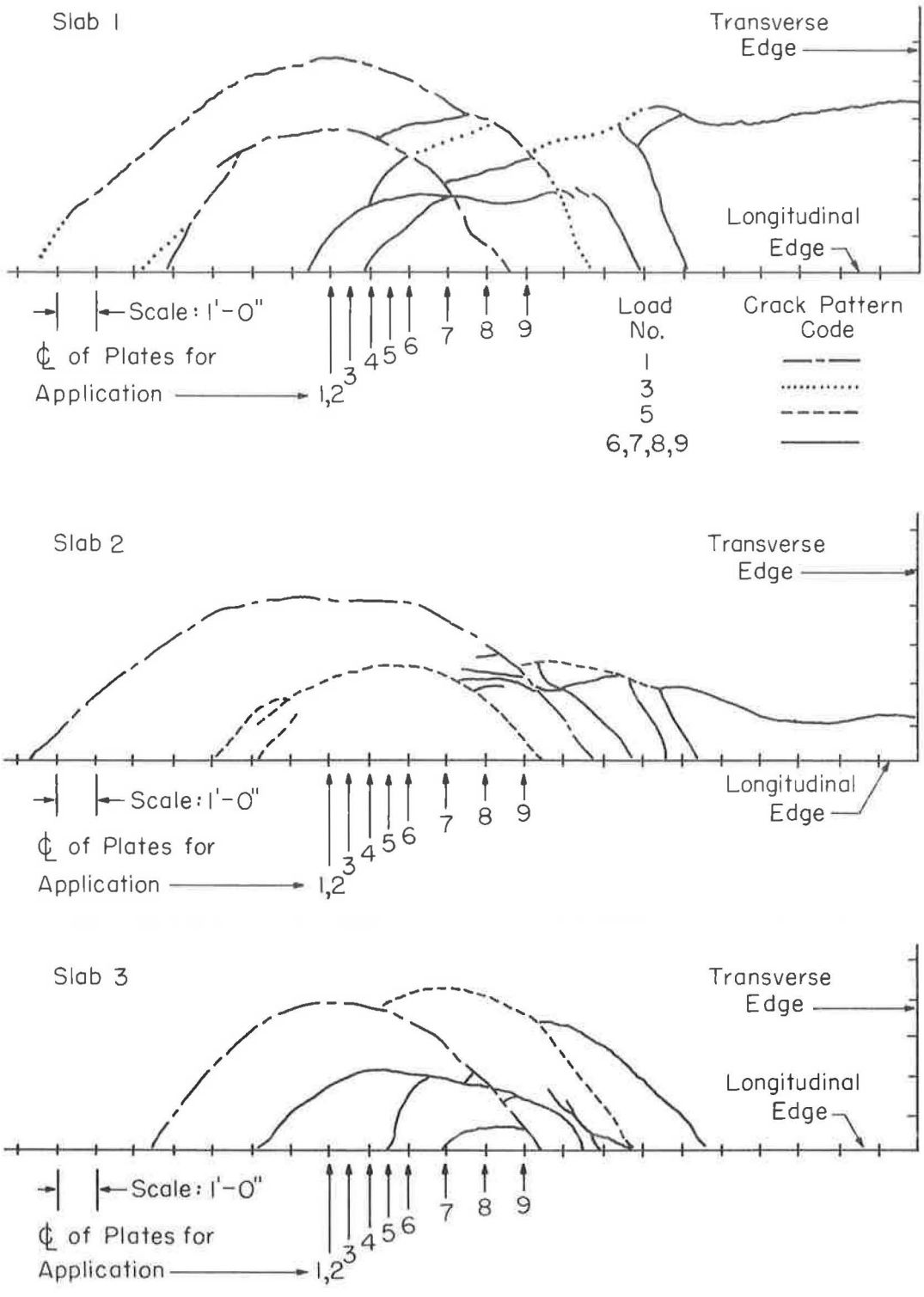

Figure 24. Top surface crack patterns for edge load tests.

slab edge adjacent to the load (Fig. 19). Averaging the data for the three slabs, the maximum residual deflections were 19 percent of the initial top cracking load deflections. Deflection profiles for second load applications showed an increase in the longitudinal distance and a decrease in the transverse distance from the load to the location of zero deflection compared to initial load applications.

During the second load applications, it was observed that the ratios of deflections and maximum stresses to load were rather constant throughout the entire range (Figs. 19-23). These ratios for the second load applications were generally slightly larger than those observed before bottom surface cracking during the initial applications. A comparison of stresses and deflections at the maximum load of the two applications indicated that variations were related to gage locations. Adjacent to the load, deflections and top surface longitudinal stresses averaged 14 and 8 percent, respectively, greater for the second applications than for the initial applications on the three slabs. Inward from the edge, the maximum top surface transverse tensile stresses were somewhat less for the second load applications due to the proximity of top cracking to the measuring gages. Stresses determined at other locations averaged the same at the maximum load for the two applications. Subgrade pressures are not reported for the second load applications because the pressure cells were inoperative after the high loads of the initial applications.

Interval Loadings.—The maximum loads applied at 6- and 12-in. intervals along the edge were 4 kips greater than those initially applied to insure a number of top surface cracks. They were equal to 52, 52, and 60 kips for Slabs 1, 2, and 3, respectively. Data from these tests showed variations due to differences in the distance between cracks. Results of the fifth 6-in. interval load application on Slab 1 (Figs. 19-21) are typical of most of the tests.

The loads causing the development of new bottom surface cracks (as determined from the edge stresses) were of interest during the top cracking interval applications. Before the formation of a new bottom surface crack, the maximum bending of the slab occurred at the previous bottom surface crack. However, as shown in Figure 20, the top compressive edge stresses at the load where the new crack developed were greater for the 6-in. interval load tests than for the initial load tests. This stress increase was probably due to the permanent subgrade deformation that developed during previous loadings and the loss of slab support. As a result, the loads causing bottom surface cracking during the 6-in. interval applications were usually smaller, by as much as 13 percent, than those determined during the initial applications.

The slabs were not instrumented to measure strains inward from the edge during the interval load applications. The maximum top surface tensile stresses along the edge during the interval load applications (Fig. 21) were similar to those determined from the second load applications. The load magnitudes causing new top surface cracking were the same for both the interval and initial load tests. A new top surface crack usually progressed from a former crack to the edge of the slab (Fig. 24). The top cracks remained visible after the loads were removed, and in a few cases after a number of loads had been applied along an edge the top cracks became enlarged.

As shown by the example in Figure 19, the ratios of maximum deflection to load were nearly constant throughout the entire range of interval applications. The maximum deflections at the top surface cracking loads of the three slabs averaged 17 percent greater during the interval applications than during the initial load applications. Deflection profiles for 6-in. interval applications showed that deflections along the slab edge were greater toward the locations of previous load applications. This illustrated the influence of permanent subgrade deformation developed during previous loadings.

INTERIOR LOAD TESTS

Static loads were also applied at an interior location of each slab. The dual loading plates were positioned midway between the longitudinal slab edges at a minimum distance of 8 ft from a transverse edge. The load was increased in 4-kip increments until either top surface cracks appeared or the loading equipment's safe limit was reached. At each increment measurements were made to determine the longitudinal and trans-

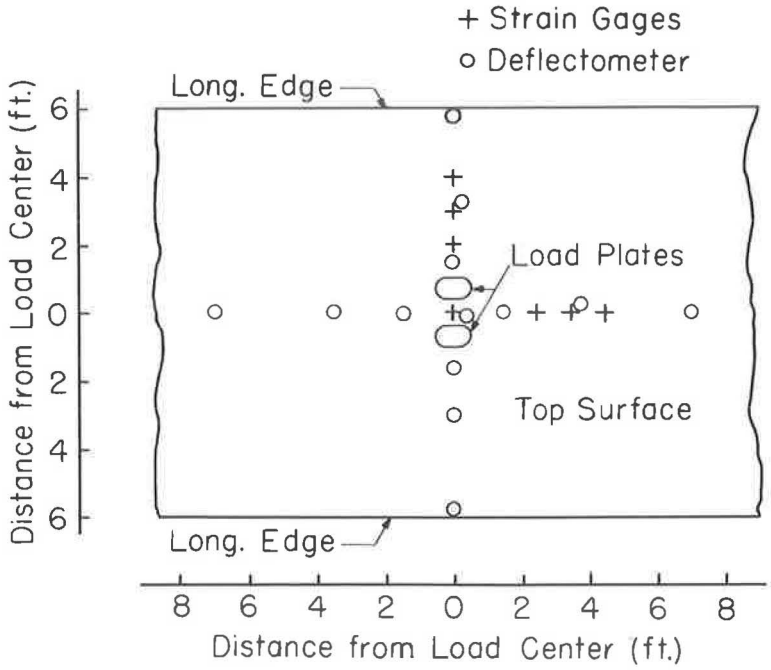

Figure 25. Interior load instrumentation plan.

verse concrete strain and deflection profiles with the instrumentation shown in Figure 25. The location of the top surface crack was also determined if one occurred.

Stresses at interior locations were computed by Eqs. 1 and 2 using the measured longitudinal and transverse strains. Top surface longitudinal and transverse compressive stresses midway between the dual loading plates are shown in Figures 26 and 27, respectively. These stresses were nearly proportional to the applied load before bottom surface cracking occurred and the transverse stress averaged 79 percent of the longitudinal stress. A comparison was made between the load test stresses prior to cracking and the values obtained using influence charts (5). For these computations, 140 pci was used for the subgrade modulus, 5 million psi for the concrete elastic modulus, and 0.15 for Poisson's ratio. The load test stresses averaged 16 percent less than the theoretical values before cracking occurred.

The magnitude of load causing bottom surface cracking was estimated from the stress diagrams shown in Figures 26 and 27. Assuming that bottom surface cracking occurred when either the top surface longitudinal or transverse compressive load stress was equal to the summation of the concrete modulus of rupture and the amount of longitudinal or transverse prestress, it was computed that the interior bottom surface cracking loads were 28.0, 26.0, and 31.2 kips for Slabs 1, 2, and 3, respectively. After cracking, the stress changes per unit load increased especially in the longitudinal direction.

Top surface cracks were visible in Slabs 1 and 2 (no transverse prestress) when interior load magnitudes were 72 and 68 kips, respectively. For each of these slabs, a longitudinal crack began between the dual loading plates and progressed to the nearest transverse edge. This was a full depth crack that probably originated as a bottom surface radial crack. It was not caused by large radial top surface tensile stresses.

No top surface cracking was observed in Slab 3 (longitudinal and transverse prestress) when a load of 100 kips was applied twice at the same interior location. A greater load could not be applied as this was the safe limit of the reaction beam and soil anchor system. As shown in Figure 28, the maximum top surface radial tensile stresses in the longitudinal direction were greater than in the transverse direction,

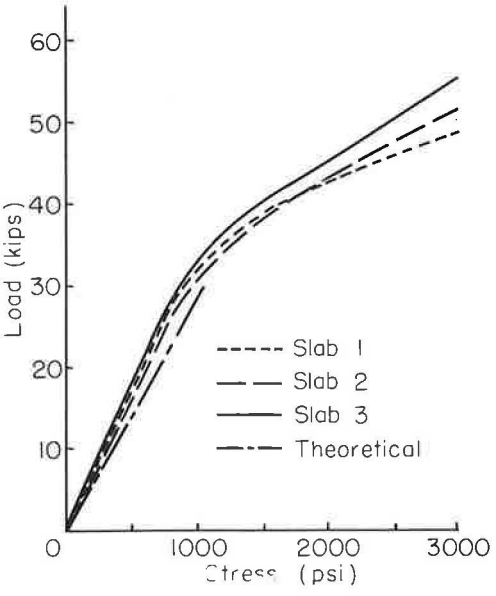

Figure 26. Top surface longitudinal compressive stress at load.

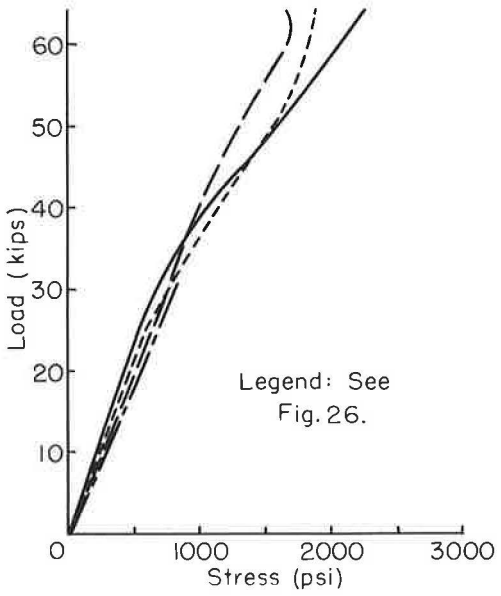

Figure 27. Top surface transverse compressive stress at load.

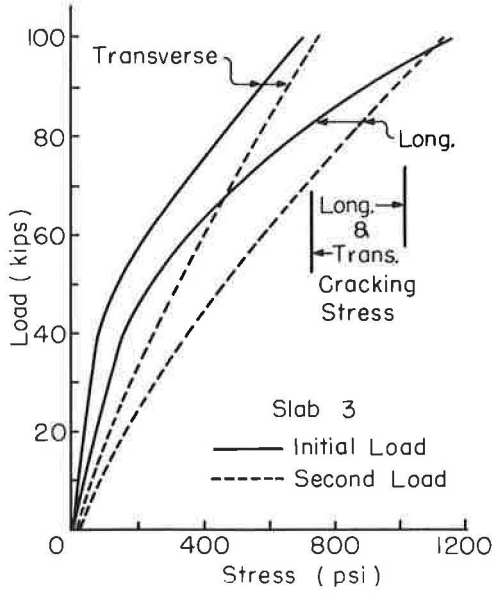

Figure 28. Maximum top surface radial tensile stress.

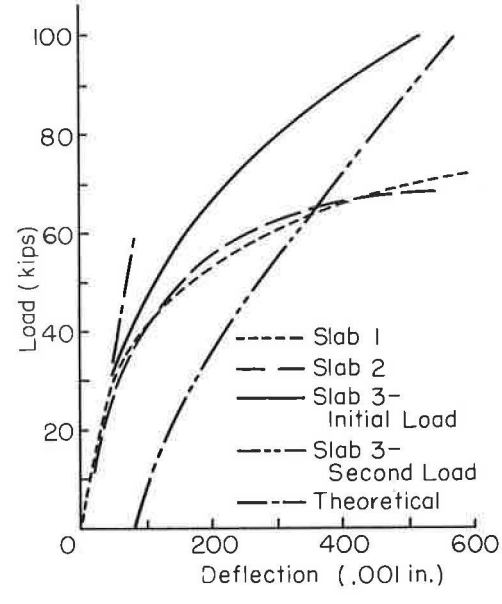

Figure 29. Interior deflection at load.

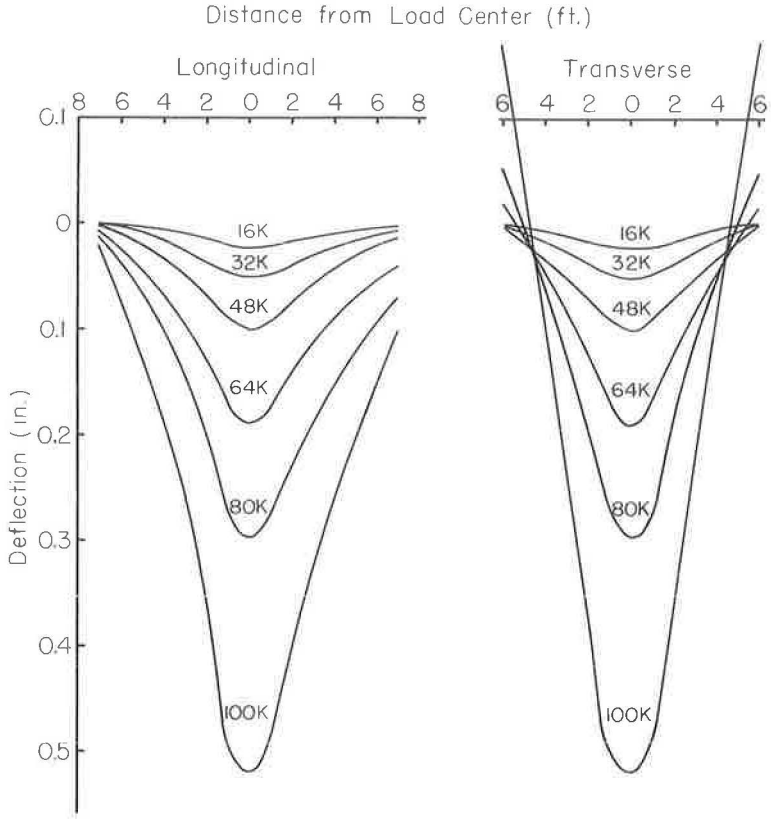

Figure 30. Deflection profiles, interior load, Slab 3.

indicating some influence from the proximity of the longitudinal slab edges. The ratios of the maximum radial tensile stresses to the applied load increased when bottom cracking occurred during the initial application but were nearly constant throughout the entire range during the second application. At a load of 100 kips, the stresses were very nearly the same for the second application as for the initial application. Assuming the cracking stress to be the summation of the concrete modulus of rupture and the amount of longitudinal or transverse prestress, it was computed from Figure 28 that top surface cracking should occur at a load near 100 kips.

The interior deflections at the load are shown in Figure 29. Prior to cracking, the measured deflections averaged 6 percent greater than the theoretical values determined from influence charts (5). After bottom surface cracking there was a progressive increase in the rate of deflection change per unit load especially for tests on Slabs 1 and 2 (no transverse prestress). After the initial load on Slab 3 was released there was a residual deflection of 0.080 in. or 15 percent of the initial 100-kip value. During the second application, the deflection to load ratio was more nearly constant throughout the entire range, and there was a 10 percent increase in the second 100-kip load deflection.

The proximity of the longitudinal slab edges influenced the load deflection profiles as shown by the typical example in Figure 30 for Slab 3 interior load increments. The longitudinal edges deflected upward at higher load magnitudes. The distances from the load to the location of zero deflection varied from about 7 to 9 ft in the longitudinal direction and from about 5 to 6 ft in the transverse direction. Obviously, the slabs were not behaving as though they were of infinite extent. No comparison was made between measured and theoretical stresses and deflections due to interior load magnitudes greater than those causing bottom cracking because the theoretical methods for determining these values assume infinite extent.

SUMMARY

The following observations apply to edge load tests:

1. The top surface longitudinal compressive edge stress at the load, the maximum top surface longitudinal tensile stress at the edge, the maximum top surface transverse tensile stress inward from the edge, and the edge deflection at the load were nearly proportional to the applied load before bottom surface cracking occurred. After cracking there were slight increases in the rate of change of these stresses and deflections per unit load.
2. Prior to bottom cracking, the edge deflection and the top surface longitudinal compressive edge stress at the load were slightly less than values determined by methods based on the elastic theory.
3. Bottom surface cracking originated at the slab edges adjacent to the load when the bottom surface tensile stress was equal to the cracking stress.
4. During load application, the maximum top surface transverse tensile stress inward from the edge was greater than the maximum top surface longitudinal tensile stress at the edge. Top surface cracking occurred when these tensile stresses were equal to the cracking stress. The top surface cracks formed initially in the longitudinal direction and progressed toward the longitudinal edge of the slab while the top cracking load was maintained.
5. When top surface cracking occurred, there was a relatively large increase in edge deflection at the load.
6. The distances from the load to the location of zero deflection varied from about 8 to 10 ft during initial applications on the uncracked slabs.
7. The ratio of the measured subgrade pressure to the slab deflection was nearly equal to the subgrade modulus determined from plate bearing tests.
8. After application and release of 24-kip loads (slightly greater than those causing bottom surface cracking in the three test slabs) the maximum residual deflections averaged 0.005 in. or 5 percent of the maximum 24-kip load deflections. After application and release of loads causing top surface cracking in the three test slabs, the maximum residual deflections averaged 0.073 in. or 19 percent of the maximum top cracking load deflections.
9. When a second load was applied after the occurrence of bottom surface cracking, the top surface longitudinal compressive edge stress at the load, the maximum top surface longitudinal tensile stress at the edge, the maximum top surface transverse tensile stress inward from the edge, and the edge deflection at the load were nearly proportional to the applied load when the magnitude was less than or equal to the maximum initially applied value. These quantities were slightly greater for equal loads than those observed before bottom surface cracking during the initial applications.
10. When loads having magnitudes sufficient to cause bottom surface cracking were applied at 6-in. intervals along the edge, the maximum bending of the slab occurred at the previous bottom surface crack until the formation of a new bottom surface crack. The loads causing bottom surface cracking during the 24-kip 6-in. interval applications were usually greater by as much as 10 percent than those that caused initial cracking. The loads causing bottom surface cracking during the 52- and 60-kip, 6-in. interval applications were usually smaller, by as much as 13 percent, than those that caused the initial cracking. There was little change in the loads causing top surface cracking during the 6-in. interval top cracking applications.

The following observations apply to interior load tests:

1. The top surface longitudinal and transverse compressive stresses midway between the dual loading plates, the maximum top surface radial tensile stresses in both a longitudinal and transverse direction from the load, and the interior deflection at the load were nearly proportional to the applied load before bottom surface cracking occurred. The ratio of transverse compressive stress to longitudinal compressive stress at the load averaged 79 percent before cracking. After cracking, there were increases in the rate of change of these stresses and deflections per unit load.

2. Prior to bottom cracking, the interior deflection at the load was slightly greater and the top surface longitudinal and transverse compressive stresses at the load were less than the values determined by methods based on the elastic theory.

3. Bottom surface cracking originated at the load when the bottom surface tensile stress was equal to the cracking stress.

4. A full depth longitudinal crack developed between the dual loading plates and progressed to the nearest transverse slab edge when an interior load averaging 2.59 times the bottom cracking load was applied to the two test slabs with only longitudinal prestress. No top surface cracks were observed in the slab with both longitudinal and transverse prestress at an interior load of 3.20 times the bottom cracking load. The maximum top surface radial tensile stresses in the longitudinal direction from the load were greater than in the transverse direction. This lack of symmetry resulted primarily from the proximity of the longitudinal slab edges.

5. Longitudinal and transverse deflection profiles also indicated that the 12-ft wide slabs did not behave similarly to one of infinite surface area when loaded at interior locations.

6. After the application and release of a load equal to 100 kips or 3.20 times the bottom cracking load on the slab with both longitudinal and transverse prestress, the maximum residual deflection was equal to 0.080 in. or 15 percent of the maximum 100-kip load deflection. When the load was applied for the second time at the same location, the top surface longitudinal and transverse compressive stresses midway between the dual loading plates, the maximum top surface radial tensile stresses in both a longitudinal and transverse direction from the load, and the interior deflection at the load were nearly proportional to the applied load for the entire 100-kip range. These quantities were greater for equal loads than those determined before bottom surface cracking during the initial application.

INTERPRETATION OF RESULTS

The three test slabs reacted similarly during initial load applications. An increase in the amount of longitudinal prestress resulted in an increase in the load causing bottom surface cracking during edge applications. The use of both longitudinal and transverse prestress resulted in an increase of the load causing bottom surface cracking during interior applications and the load causing top surface cracking during edge applications on the two slabs with only longitudinal prestress; whereas, no top cracking was observed in the slab with both longitudinal and transverse prestress when the interior load was equal to the highest magnitude obtainable with the loading equipment.

Bottom surface cracks did not develop into full depth cracks during any edge load test at intervals of 6 in. along the longitudinal edges of all three slabs or during the interior load test of the slab with both longitudinal and transverse prestress. Bottom surface cracking had no apparent detrimental effect on the ability of the three slabs (including the two with only longitudinal prestress) to support the edge loads applied in the test program. Bottom surface cracking also had no apparent detrimental effect on the ability of the test slab with both longitudinal and transverse prestress to support an interior load.

When top surface cracking occurred during an edge load application, there was a large increase in slab deflection at the load. The top cracks remained visible after the loads were removed, and after a number of loads had been applied along an edge there was a general deterioration of the pavement and subgrade. There was also a large increase in slab deflection at the load when a full depth longitudinal crack occurred during interior load application on each of the two slabs with only longitudinal prestress. This crack, which probably originated as a bottom surface radial crack, was visible in the top surface at a load much greater than that causing bottom surface cracking during the single static load application. It seems likely that this full depth crack might occur at a load close to that causing bottom surface cracking during repeated moving load applications. Therefore, until additional information is obtained on the effect of traffic conditions, load applied at interior locations of a concrete highway or airfield pavement prestressed only in the longitudinal direction might be limited to that causing bottom surface cracking.

The results of the load test program therefore suggest that the criterion for failure of a prestressed pavement is occurrence of a top surface crack. Bottom surface cracking may be allowed if prestress is applied properly to prevent the bottom cracks from developing into full depth cracks. With this criterion for failure, a prestressed concrete pavement can support a substantially greater load than a conventional concrete pavement of the same thickness. Part of this additional load capacity is due to the increase in allowable stress causing pavement cracking by the amount of prestress applied to the pavement in a direction perpendicular to the cracking. Most of the additional load capacity is a result of the allowance of loads greater than those causing bottom surface cracking. Therefore, the load-carrying advantage obtained by prestressing a concrete pavement is due principally to a change in the criterion for failure from a bottom surface crack to a top surface crack. This justified change in failure criterion has more significance than the amount of prestress that is applied.

In the design of a prestressed concrete pavement it is necessary to determine whether prestress should be applied in more than one direction. To fully utilize the load-carrying advantage obtained by prestressing, the prestress should be applied in directions that make it possible to allow bottom surface cracking. The results of the static load test program suggest that to allow the application of bottom surface cracking loads, two-directional prestress is necessary for interior load applications but longitudinal, prestress is sufficient for edge load applications. Another advantage obtained by prestressing a concrete pavement is the elimination of weakened plane type transverse contraction joints. This is accomplished by applying sufficient prestress to overcome pavement tensile stresses that result from subgrade friction, warping, curling, and a nonlinear temperature or moisture differential throughout the depth of a pavement. Both concrete airport and highway pavements will require longitudinal prestress to reduce the number of transverse joints. Airport pavements may require transverse prestress to allow the application of interior loads greater than those causing bottom surface cracking.

While both longitudinal and transverse prestress may be required for airport pavements, it may be possible and also desirable for reasons of economy to construct a prestressed concrete highway pavement with only longitudinal prestress. Transverse prestress may not be needed to obtain a joint-free pavement or to allow the application of loads greater than those causing bottom surface cracking at edge locations. The maximum load on a concrete highway pavement prestressed only in the longitudinal direction is probably limited to that causing bottom surface cracking when applied at interior locations. If two-directional prestress is used, the maximum load is probably limited to that causing top surface cracking when applied at edge locations. Therefore, the use of transverse as well as longitudinal prestress results in a further increase in load-carrying capacity. This factor should be considered in deciding whether transverse prestress is worthwhile in a concrete highway pavement.

It should be emphasized that only half-axle conditions were represented in the test program. No attempt was made to combine stresses and deflections for full axle conditions. Only static load tests were conducted, and the conclusions may be subject to some modification when the effects of repeated traffic loads are considered especially in the determination of the failure criterion.

REFERENCES

1. Carlton, P. F., and Behrmann, R. M., "Model Studies of Prestressed Rigid Pavements for Airfields." HRB Bull. 179, pp. 32-50 (1958).
2. Moreell, B., Murray, J. J., and Heinzerling, J. E., "Experimental Prestressed Concrete Highway Project in Pittsburgh." HRB Proc. 37:150-193 (1958).
3. Hanson, N. W., "Load Cells for Structural Testing." Jour. of PCA Res. and Dev. Labs., PCA Dev. Dept. Bull. D33 (Jan. 1959).
4. Carlson, R. W., and Pirtz, D. G., "Development of a Device for the Direct Measurement of Compressive Stress." ACI Proc. (Nov. 1952).
5. Pickett, G., Raville, M. E., Janes, W. C., and McCormick, F. J., "Deflections, Moments and Reactive Pressures for Concrete Pavements." Bull. 65 and Supplement, Kansas State College Experimental Station (Oct. 1951).